



## Research Article

# Cardioprotective Efficacy of Silymarin Liquisolid in Isoproterenol Prompted Myocardial Infarction in Rats

Nermin M. Sheta,<sup>1,4</sup> Yasmin A. Elfeky,<sup>2</sup> and Sylvia A. Boshra<sup>3</sup>

Received 19 August 2019; accepted 12 December 2019; published online 23 January 2020

**Abstract.** Myocardial infarction (MI) is the principal cause of death in many countries. Silymarin (SM) is a herbal antioxidant and can be efficiently used in preventing cardiovascular diseases (CVDs). The study is aimed to enhance the absorption rate and biological activity of SM by using liquisolids besides investigating the cardioprotective activity of SM and its selected liquisolid formula against isoproterenol prompted cardiotoxicity in rats. Eight formulae were prepared according to (2<sup>3</sup>) full-factorial design. The effect of viscosity increasing agent type and concentration, as well as the carrier/coat ratio on the dissolution rate and angle of repose were studied. All formulae were tested for content uniformity, micromeritic properties, dissolution performance besides the evaluation of its physicochemical properties, and scanning electron microscopy (SEM). Based on the factorial design outcomes, the highest desirability was obtained from F3 with excipient ratio value (R) of 20%, dissolution rate at Q<sub>5 min</sub> of 26.9%, and angle of repose of 19. Oral administration of F3 liquisolid and SM revealed a significant protective efficacy against the modification of cardiac plasma markers, brain natriuretic peptide (BNP), interleukin-10 (IL-10), vascular endothelial growth factor (VEGF), and transforming growth factor (TGF)-β1 besides cardiac superoxide dismutase (SOD), malondialdehyde (MDA), and total protein kinase-1 (Akt-1) levels. Additionally, they minimized cardiac inducible nitric oxide synthase (iNOS), microRNA-34a (miR-34a), and p38 mitogen-activated protein kinase (p38-MAPK) levels. In conclusion, F3 liquisolid compact possessed an overall pronounced results over pure SM reckoned to its enhanced solubility and efficacy.

**KEY WORDS:** silymarin; liquisolid; micromeritic properties; isoproterenol; microRNA-34a.

## INTRODUCTION

*Silybum marianum* is a milk thistle herb comprising a blend of various flavonolignan and flavonoids (1). The active blend is composed of four flavonolignan isomers known as silymarin (SM). Silybin (A and B) is the primary and most active component and makes up to 50–70% of SM (2). The main drawback of SM is its poor solubility (0.04 mg/mL); for that reason, many approaches had been taken to enhance its solubility and in turn its bioavailability. SM retains no lipophilic properties, in spite of its poor solubility in water (3). SM has anti-inflammatory and anticarcinogenic properties leading to its use in the treatment of different liver, cardiovascular diseases (CVDs) (4), and certain types of cancer (2).

SM is an herbal antioxidant which is ten times more potent than other antioxidants, e.g., vitamin E (5). SM increases the stability of membrane and helps in the regeneration of tissues. SM prevents cardiac diseases through numerous mechanisms which include chelating promoters of metals and scavenging free radicals, preventing the formation of reactive oxygen species (ROS) enzymes, activating antioxidant enzymes and inhibiting lipid peroxidation (6), regulating the permeability of the cell membrane and increasing its stability (7).

Isoproterenol has a positive inotropic and chronotropic effect and is considered as a synthetic catecholamine. It increases cardiac output at therapeutic doses, but when administered in large doses, it causes severe oxidative stress in the myocardium causing the death of the left ventricular of the heart muscle. The mechanistic pathway *via* which isoproterenol induces necrosis was believed to take place through the generation of free radicals which mediates oxidative stress (8).

Orally administered SM is absorbed rapidly with a  $t_{max}$  between 2 and 4 h and  $t_{1/2}$  of 6 h. Only 20 to 50% of oral SM is absorbed as it undergoes extensive first pass effect from the

<sup>1</sup>Pharmaceutics Department, Faculty of Pharmacy, O6U, 6th of October City, Central Axis, Part 1/1, Behind Sixth October City Authority, Giza, Egypt.

<sup>2</sup>Pharmaceutics Department, Faculty of Pharmacy, MTI, Cairo, Egypt.

<sup>3</sup>Biochemistry Department, Faculty of Pharmacy, O6U, Giza, Egypt.

<sup>4</sup>To whom correspondence should be addressed. (e-mail: nerminsheta@o6u.edu.eg)

gastrointestinal tract (GIT). Therefore, absorption of SM from the GIT is low (9), impacting its oral bioavailability (3). This limitation in SM bioavailability might be attributed to four main causes: 1<sup>st</sup> is the extensive phase effect, 2<sup>nd</sup> is the low intestinal permeability, 3<sup>rd</sup> is its poor aqueous solubility, and 4<sup>th</sup> is due to its rapid excretion in bile and urine (3).

Several methodologies for increasing SM oral bioavailability have been studied broadly through co-solvency, complexation, and also *via* targeted drug delivery systems, *e.g.*, a transdermal delivery for different skin-related disorders like skin cancers, all these methods can lead to a greater *in vivo* drug performance (3,10,11).

Liquisolid technique is considered as an advanced method for enhancing drug dissolution. The principle of liquisolid drug delivery is to convert liquid medication into dry, non-sticky, free flowing, and compressible powder form, by mixing the liquid medications with suitable excipients termed as carriers and coating materials (12).

Liquisolid technique is not applicable to achieve high drug loading as they require large amount of carrier and coating material to convert the liquid medication into free-flowing powder with acceptable compressibility properties resulting in increase in tablet weight impacting its swallowability. Several strategies have been reported to overcome this obstacle, by adding some additives such as polyvinylpyrrolidone (PVP), hydroxypropyl methylcellulose (HPMC), and PEG 35000 into the liquid medications to increase its viscosity and hence reduce the quantities of carrier and coating material. By this way, low amount of carrier is needed to obtain a dry powder with good flowability and compactibility properties (12,13).

The objective of this work was to develop a liquisolid system for improving the discounted oral absorption and efficacy of the poorly water-soluble SM as a cardioprotective; this might make a breakthrough as a new approach to protect other organs in addition to liver. The improved efficacy of SM as cardioprotective was assessed through the biological and biochemical tests against isoproterenol-induced cardiotoxicity in adult rats.

## MATERIALS AND METHODS

### Materials

Silymarin (kindly obtained from “CID” Company, Egypt); hydroxypropyl methylcellulose K4M (HPMC K4M) (4000 cps) (Sigma-Aldrich Co., Germany); isoproterenol and propranolol (Merck, Germany); polyvinylpyrrolidone K30 (Merck, Germany); propylene glycol (PG), glycerin, polyethylene glycol 200 (PEG) (Fluka, Switzerland); Cremophor<sup>®</sup> RH40 and Cremophor<sup>®</sup> EL (BASF, Germany); Tween 80 (Merck-schuchardt, Germany); Labrafil<sup>®</sup>, Capryol 90<sup>®</sup> and transcutool (Gattefosse, France); Avicel<sup>®</sup> PH 102 (MCC PH102) and Aerosil<sup>®</sup> 200 (colloidal silicon dioxide) were supplied by FMC Biopolymer Corp., USA.

### Solubility Study

To select the most appropriate liquid vehicle to dissolve SM, a solubility study was carried out in various liquid vehicles, namely, Cremophor<sup>®</sup> RH40, Cremophor<sup>®</sup> EL, PG, glycerin,

PEG 200, Tween 80, Capryol 90<sup>®</sup>, Labrafil<sup>®</sup>, transcutool, and distilled water. Solutions were prepared by adding excess amount of SM in the previously mentioned liquid vehicles. The mixtures were continuously stirred using vortex for 10 min and kept at  $25 \pm 0.5^\circ\text{C}$  in water bath shaker (model 25, Precision Scientific, Chicago) for 72 h till reaching equilibrium. These samples were then centrifuged at 5000 rpm for 10 min followed by filtration of the supernatant through 0.45  $\mu\text{m}$  membrane filter (14,15). The filtered supernatants were suitably diluted with PB saline pH 6.8 and analyzed using UV spectrophotometer (UV-1601 PC, Shimadzu, Japan) at the predetermined  $\lambda_{\text{max}} = 285.8 \text{ nm}$  (16).

### Factorial Design

A full-factorial design ( $2^3$ ) was constructed in this study using Design expert 8.0.7 software (StatEase Inc., USA). The studied factors were as follows: the viscosity increasing agent type ( $X_1$ ), the viscosity increasing agent concentration ( $X_2$ ), and the carrier/coat ratio ( $X_3$ ). Levels for each variable were determined as indicated in Table I. The design aimed to investigate the combined effect of these factors on the angle of repose ( $Y_1$ ) and percent of drug dissolved after 5 min (%  $Q_{5 \text{ min}}$ ) ( $Y_2$ ). Eight experimental runs were prepared in triplicate, and all data were statistically subjected to analysis of variance and were considered significant at  $p < 0.05$ .

### Load Factor Calculation

In a liquisolid system, the amount of liquid taken by the carrier and coating materials depends on the excipient ratio (R), which is defined as the ratio between the weights of carrier (Q), and coating ingredients (q) present in each formula (17). Preparation of a liquisolid system with an acceptable flow and compressibility is possible when the maximum amount of retained liquid for the carrier material is used and not exceeded (18). This characteristic amount of liquid is called liquid load factor ( $L_f$ ), which equals the weight ratio of the liquid drug (W)/ the carrier powder (Q) in a system. To calculate the loading factor, PG was added to 10 g carrier and mixed for 1 min. This procedure was repeated till obtaining a system with acceptable flow rate (17).

**Table I.** Full-Factorial ( $2^3$ ) Design for the Preparation of SM Liquisolid

Factors	Levels
X1*	HPMC K4M      PVP K30
X2**	20%              40%
X3***	5:1                20:1
Response	Desirability
$Y_1$ (angle of repose)	Lowest
$Y_2$ (% drug dissolved after 5 min)	Highest

\* $X_1$ : viscosity increasing agent type

\*\* $X_2$ : viscosity increasing agent concentration

\*\*\* $X_3$  R value (carrier:coat ratio)

### Preparation of SM Lisquisolid Free-Flowing System

The formulation design of lisquisolid was done in accordance with the mathematical model defined by Pavani *et al.* (19). In this study, the liquid vehicle was used according to the results of saturated solubility study. PVP K30 or HPMC K4M was used as a viscosity increasing agent in two different concentrations according to the mentioned factorial design. The liquid/drug solution was produced by mixing SM with PG in a beaker. To this liquid/drug mixture at which drug is totally soluble, the calculated amount of the viscosity increasing agent was added gradually, then carrier (Avicel® PH102) was added gradually, with constant stirring with intermittent break off to release lumps from the edges of the container by scraping with a spatula, then the calculated amount of Aerosil® 200 was added with continuous stirring until a free-flowing system was obtained, carrier/coat ratio (R) used was either 5 or 20. The compositions of the prepared SM lisquisolid free-flowing powder are shown in Table II.

### Preparation of SM Lisquisolid Capsules

The direct filling technique was applied for the preparation of SM lisquisolid capsule, with which the pre-sieved bulk lisquisolid powder was loaded into it without granulation. Free-flowing SM lisquisolid powder (0.5 g) containing 40 mg SM was filled into hard gelatin capsule size 00 (20).

### Characterization of the Prepared SM Lisquisolid Free-Flowing Powder

#### Content Uniformity

To determine whether the drug was uniformly distributed within the formulated lisquisolid, a specified amount lisquisolid powder with calculated amount of drug was taken randomly. Powder was dissolved in PB saline pH 6.8, and sonicated for 15 min, filtered through 0.2 µm Millipore filter,

then measured using UV spectrophotometer at the predetermined  $\lambda_{\max} = 285.8$  nm (16). The percentages of individual drug content were calculated against the average drug content, according to the British Pharmacopoeia (2012) (21). The drug content should be in the range of 85 to 115% in order to confirm the uniformity of drug content during mixing with the rest of excipients.

#### Micromeritics Properties

All lisquisolid compacts were exposed to precompression studies which were done by fixed funnel and free-standing cone method adopted by Kamel and Basha (2013) (22). The angle of repose (°) was given by  $\tan^{-1} h/r$ , Carr's index and Hausner's ratio was calculated from the bulk and tapped density of the final blends (23). Percentage compressibility was calculated as follows:

$$\text{Carr's index} = \frac{\rho_p - \rho_b}{\rho_p} \times 100 \quad (1)$$

The Hausner's ratio was calculated as follows (24):

$$\text{Hausner's ratio} = \frac{\text{volume before tapping}}{\text{volume after tapping}} \quad (2)$$

#### Dissolution Study

The USP paddle method operated at 100 rpm (USP dissolution, apparatus II, Pharma Test, Germany) with PB saline pH 6.8 was used as its dissolution medium (25). The capsules containing either SM free-flowing lisquisolid powder or pure SM (26,27) were placed at the bottom of the cell using a capsule sinker to avoid its floating in 500 mL medium at  $37 \pm 0.5^\circ\text{C}$  compared to SM free drug of the same concentration. At appropriate intervals (5, 10, 15, 20, 25, 30, 35, 40, 45, 50, 55, 60 min), 5 mL samples were withdrawn and filtered through 0.2 µm Millipore filter and replaced with fresh medium. The samples were measured spectrophotometrically at the predetermined wavelength  $\lambda_{\max} = 285.8$  nm (16). The mean

**Table II.** Composition of the Prepared SM Lisquisolid Free-Flowing Powder and Its Micromeritic Properties

Constituents mg	Formulae code							
	F1	F2	F3	F4	F5	F6	F7	F8
Silymarin	80	80	80	80	80	80	80	80
PG	300	300	300	300	300	300	300	300
HPMC K4M	–	–	–	–	120	60	120	60
PVP K30	120	60	120	60	–	–	–	–
Avicel® PH102	433.3	433.3	495.2	495.2	433.3	433.3	495.2	495.2
Aerosil® 200	86.7	86.7	24.8	24.8	86.7	86.7	24.8	24.8
Formula no.	Micromeritic properties (mean average value, $n = 3$ )					Hausner's ratio	Angle of repose (°)	
	$\rho_b$ (g/cm <sup>3</sup> )	$\rho_p$ (g/cm <sup>3</sup> )	CI (%)					
F1	0.35	0.41	14.60	1.17		22		
F2	0.35	0.40	12.50	1.18		31		
F3	0.44	0.50	12.00	1.11		19		
F4	0.37	0.42	11.90	1.21		27		
F5	0.22	0.37	22.40	1.31		34		
F6	0.31	0.40	22.50	1.32		40		
F7	0.33	0.41	19.30	1.21		30		
F8	0.34	0.43	20.90	1.40		38		

value of three determinations was used to calculate SM release from each formulae and statistical analysis of dissolution data was performed to demonstrate the impact on drug release.

### Characterization of the Selected SM Liquisolid Free-Flowing Powder

The selected SM liquisolid compact giving the highest desirability with lowest angle of repose value and highest dissolution percent at  $Q_{5\text{ min}}$  was subjected for the following tests:

#### DSC

The differential scanning calorimetry (DSC) studies for SM and the selected liquisolid compact were done by DSC (50, Shimadzu, Japan). It was carried out by placing samples of 3–4 mg in aluminum pan then heated at the rate of 10°C/min to a temperature of 200°C. Dry nitrogen gas with a flow rate of 25 mL/min was used as a carrier gas to purge the cell.

#### FT-IR

The Fourier transform infrared spectroscopy (FT-IR) spectrum for SM and the selected liquisolid compact was performed separately by mixing each sample with KBr at a ratio of 2:200 (tested substance: KBr), and the samples were directly loaded into FT-IR (IRAffinity-1, Shimadzu, Japan) in the frequency of 4500–500  $\text{cm}^{-1}$ .

#### XRD

The angle of diffraction gives an indication of crystalline or amorphous nature of the main active constituent. X-ray powder diffraction (XRD) patterns were determined for SM and the selected liquisolid compact. The X-ray diffraction was obtained using Advanced Diffraction system (Scintag Inc., USA) with a copper target at a voltage of 40 kV and a current intensity of 30 mA at a scanning speed of 1°C/min.

#### SEM Topographic Visualization

Topographic visualization by scanning electron microscopy (SEM) is performed to evaluate the surface characteristics of SM and the selected liquisolid compact. The samples were placed on a carbon tape. The samples were sputter coated with gold for 120 s followed by examination under microscope (QUANTA FEG 450) at a voltage of 20 kV under different magnification power.

## INVESTIGATING THE CARDIOPROTECTIVE EFFICACY OF SM IN ISOPROTERENOL PROMPTING MYOCARDIAL INFARCTION IN RATS

### Experimental Animals

This experiment was conducted under the guidelines of the animal care and use committee of Faculty of Pharmacy, O6U, Egypt. Forty rats ( $180 \pm 10$  g) were brought from the National Cancer Institute of Cairo University and were separately placed in an air-conditioned cages at a temperature of  $22 \pm 2^\circ\text{C}/60\%$  RH with an 8:00 to 20:00 light cycle.

During the accommodation, each animal was raised up on a regular diet *ad libitum*.

### Experimental Design

The biochemical effects of SM and the selected liquisolid formula on rats with induced myocardial infarction were studied. Five groups of animals each of 8 rats were treated everyday as follows:

Group (1): Control group was given normal diet for 15 days.

Group (2): Positive control was given isoproterenol (85 mg/kg) suspended in saline subcutaneously on the 14<sup>th</sup> and 15<sup>th</sup> day (28).

Group (3): Treated with propranolol (10 mg/kg, orally) daily for 15 days (29) + isoproterenol (85 mg/kg, orally) suspended in saline subcutaneously on the 14<sup>th</sup> and 15<sup>th</sup> day.

Group (4): Treated with SM (100 mg/kg, orally) daily from day 6 to day 15 + isoproterenol (85 mg/kg, orally) suspended in saline subcutaneously on the 14<sup>th</sup> and 15<sup>th</sup> day.

Group (5): Treated with F3 SM liquisolid (100 mg/kg, orally) daily from day 6 to day 15 + isoproterenol (85 mg/kg, orally) suspended in saline subcutaneously on the 14<sup>th</sup> and 15<sup>th</sup> day.

At the end of the experiment, rats were sacrificed and the blood was collected, centrifuged, and the plasma was used for the measurement of creatine kinase (CK-MB) according to Gerhardt and Waldenström (1979) method (30), plasma lactate dehydrogenase (LDH) according to King (1965) method (31) as well as the levels of cardiac troponin T (cTnT) and B-natriuretic peptide (BNP) were determined with the kit of ELISA according to the instructions of the manufacturer (R&D Systems Inc., Minneapolis, USA) in plasma. Also, serum interleukin-10 (IL-10), vascular endothelial growth factor (VEGF), and transforming growth factor (TGF)- $\beta$ 1 were determined by ELISA technique using standard kits from RayBiotech, Inc., USA; Quest Diagnostics Nichols Institute, San Juan Capistrano, CA; and R&D Systems Inc., Minneapolis, MN, USA, respectively. Cardiac superoxide dismutase (SOD) and malondialdehyde (MDA) were measured by the methods adopted by Nichans and Samulelson (32) and Marklund and Marklund (33), respectively. In addition, cardiac level of total protein kinase-1 (Akt-1) was determined by ELISA technique using standard kits (RayBiotech, Inc., GA).

### Western Blot

Samples of hearts were taken from each group after 3 min of the last administration. Lysis buffer was added for 1 h and then centrifuged at  $16,009.2 \times g$ . The tissue protein concentration in the supernatant was determined by bicinchoninic acid (BCA) method, and isolation of  $\beta$ -actin, iNOS, and p38 MAPK was done by 10% SDS-PAGE gel electrophoresis. The proteins were put onto PVDF membrane for 2 h then washed with Tris buffer saline Tween (TBST) for 5 min and then blocked with TBST blocking buffer containing 5% skim milk powder for 1 h. Then, the blocking buffer was discarded. The first antibodies of iNOS



(1:1000),  $\beta$ -actin (1:1000), and p38 MAPK (1:1000) were added onto the membrane, respectively, and incubated overnight at 4°C and then washed with TBST (five times) for 5 min; the second antibody (HRP goat anti-rabbit IgG (H+L), 1:2000) was added and incubated for 2 h and then washed for five times with TBST for 5 min each time, and finally, enhanced chemiluminescence (ECL) color solution was added.

### MiRNA-34a Analysis Using RT-qPCR

Total RNA from myocardial tissue was extracted by TRIzol reagent (Invitrogen, CA, USA), its concentration was measured by UV spectrophotometer, and the integrity was analyzed by gel imaging system (Bio-Rad Laboratories, Inc., Hercules, CA, USA). Reverse transcription reaction was accomplished with mi-RNA specific RT primer (GenScript USA Inc., Nanjing, China) using the kit of reverse transcription polymerase chain reaction (MBI Fermentas, the Republic of Lithuania). Mature miR-34a primers were synthesized by GenScript Co. Ltd. (China). The primers were as follows: forward (5'-TGCG CTGGCAGTGTCTTAGCTG-3') and reverse (5'-CCAG TGCAGGGTCCGAGGTATT-3'), both were detected by Taqman mi-RNA assay probe (Applied Biosystems, Shanghai, China) and normalized by endogenous U6 small RNA. Reverse transcription was done according to the following conditions: 37°C (15 min), 42°C (50 min), and 85°C (5 min). The cDNA was subjected to real-time PCR under the following conditions: 50°C (2 min), 95°C (10 min), 95°C (5 s), and 60°C (30 s).

### Statistical Analysis

All the grouped data were statistically evaluated using SPSS 15 software (Inc., Chicago, IL, USA, 2012). The comparison between groups included one-way analysis of variance (ANOVA) followed by the least significant difference test.

## RESULTS AND DISCUSSION

### Solubility Study

The solubility of SM in Cremophor® RH40, Cremophor® EL, glycerin, PEG 200, PG, Tween 80,

**Table III.** Silymarin Solubility in Various Liquid Vehicles

Vehicle	Solubility (mg/mL)
Distilled water	0.034
Cremophore® RH40	18.228
Cremophore® EL	12.551
Glycerin	7.478
PEG 200	282.221
PG	308.600
Tween 80	14.738
Labrafil®	2.075
Capryol 90®	2.740
Transcutol	267.999

Data are presented as mean average value,  $n = 3$

Capryol® 90, Labrafil®, transcutool, and distilled water is given in Table III. The solubility of SM in PG was significantly ( $p < 0.0001$ ) greater in comparison with other liquid vehicles. The higher segment of SM in PG was in the solubilized form in comparison with other vehicles, and this would help to increase the dissolution of SM (12). Hence, PG was selected as a vehicle for SM liquisolid preparation.

### Load Factor Calculation

From literature, it was shown that the traditional liquisolid tablet preparation with good flowability and compactibility was found to be difficult when the loading factor was  $> 0.25$ . Preparing systems using PVP and HPMC could increase the liquid adsorption capacity of the liquid medication (34), enabling  $L_f$  to increase  $> 0.25$  (13). In the current study, by using PVP K30 and HPMC K4M in concentration of 20% or 40%, the  $L_f$  value was found to be 0.57, and still, these formulations could hold good flow properties. According to the previously mentioned equation ( $L_f = W/Q$ ),  $L_f$  is inversely proportional to the amount of carrier needed in the formulation. Consequently, the higher the  $L_f$ , the less was the amount of carrier and coat material essential to produce dry, non-sticky, with good flow properties, and readily compactible liquisolid formulae (35).

### Characterization of the Prepared SM Liquisolid

#### Content Uniformity

Drug content of all the formulae was between  $98.56 \pm 0.98$  and  $102.89 \pm 1.03\%$  of the claimed quantity; this confirms the uniform drug content and proper mixing of drug with the rest of the excipients (36).

#### Micromeritic Properties

The flow characteristics of SM liquisolid formulae are shown in Table II. It is known that value of  $56^\circ$  shows very poor flow, values of  $31$  to  $35^\circ$  show good flow, values of  $36$  to  $40^\circ$  or  $41$  to  $45^\circ$  indicate passable flow, and with values of  $46$  to  $55^\circ$  (37) indicate a poor flow which require agitation or vibration.

Studying the effect of different independent factors on values showed that F3 had an excellent flow with the lowest of 19, CI% of 12%, and Hausner's ratio of 1.11. Figure 1 portrays the effect of different factors on the angle of repose. Using either HPMC or PVP was found to have a significant ( $p < 0.0001$ ) effect on . The presence of PVP was found to have a significant lower value for when compared to those prepared with HPMC as seen in Fig. 1a. This was in accordance with Nokhodchi *et al.* (38) who used liquisolid as an approach to sustain the drug release and observed that HPMC had an outstanding effect on the mechanical characteristics of the liquisolid tablets, while the presence of PVP was found to have a significant lower value for compared to those prepared with HPMC.

As in Fig. 1b, the flowability of powders was improved ( $p < 0.0001$ ) as the amount of PVP in drug-vehicle mixture increased; this resulted in the increase of the amount of the carrier and coating materials. The increased viscosity of the drug-vehicle mixture with the increase of PVP level made less carrier and

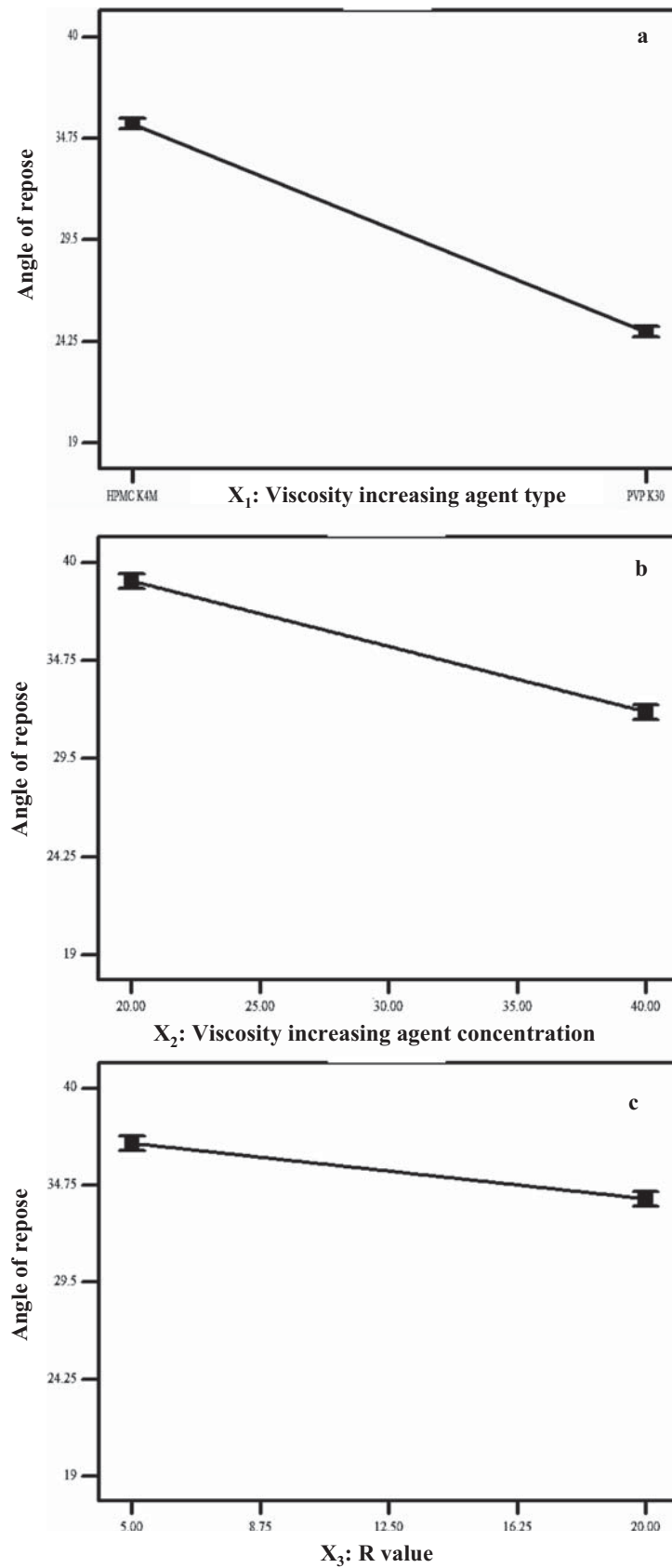


**Fig. 1.** The effect of **a** X<sub>1</sub> (viscosity increasing agent type), **b** X<sub>2</sub> (viscosity increasing agent concentration), and **c** X<sub>3</sub> (R value) on angle of repose

coating materials needed to completely adsorb liquid. Therefore, powder flowability was improved due to relatively large proportion of carrier and coating materials used (39).

SM liquisolid formulae containing high quantity of Aerosil® 200 (R=5) were fluffy owing to its low density (0.05 g/mL). As revealed in Fig. 1c, the presence of high amount of Aerosil® 200 in the formulae resulted in a significant decrease in the powder flow properties ( $p < 0.0001$ ), whereas the formulae prepared with higher excipient ratio (R = 20) showed a significant improved flow properties ( $p < 0.0001$ ) due to the enhanced amount of Avicel® PH 102 (40).

Also, Jaipakdee (41) explained this finding due to the low R values contained small amounts of Avicel® PH 102, and large amounts of colloidal silica. Avicel (microcrystalline cellulose, MCC) is a highly hygroscopic material widely used as flowability aid, diluent, and disintegrant. MCC also enhances liquid transport into a tablet matrix, accelerating both diffusion and capillary action (42). On the other hand, colloidal silicon dioxide possess poor compressibility and hydrophobic property (34); these findings were in accordance with Spireas and Komala (43,44).

### Dissolution Study

The profiles of the drug dissolution from the prepared liquisolid capsules and from pure SM capsules in PB saline pH 6.8 are shown in Fig. 2. F3 liquisolid capsule showed the highest dissolution profile, and a high amount of SM was dissolved immediately after 5 min (%  $Q_{5 \text{ min}}$ ) of 26.9%, with nearly a complete SM dissolution within 60 min (%  $Q_{60 \text{ min}}$ ) of 98%, while the pure SM indicated 1.8% at  $Q_{5 \text{ min}}$  and 9.6% at  $Q_{60 \text{ min}}$ . This indicated an obvious improvement ( $p < 0.05$ ) in the rate and extent of SM release from the liquisolid capsule as compared to the pure SM.

Surface area is typically increased by reduction in particle size; in this case, the enhanced dissolution is caused by two factors: the wettability has increased due to the presence of PG (hydrophilic material) and the form conversion from crystalline to amorphous state. The solubility of SM liquisolid formulae in the dissolution medium was increased in spite of the small amount of liquid vehicle, which was sufficient to increase the solubility of SM liquisolid particles

by acting as a co-solvent with the dissolution medium. Consequently, the concentration gradient of SM liquisolid and its dissolution rate were increased (39,45).

The effect of different studied factors on the %  $Q_{5 \text{ min}}$  is shown in Fig. 3a, b, and c revealed that the type of viscosity increasing agent had an obvious ( $p < 0.0001$ ) effect on the drug dissolution from SM liquisolid capsules. Using HPMC as a viscosity increasing agent caused a significant decrease in the dissolution rate of the SM from the liquisolid capsule. Likewise, F1, F2, F3, and F4, prepared using PVP as a viscosity increasing agent, showed %  $Q_{5 \text{ min}}$  of 20.4, 17, 26.9, and 18%, respectively, while F5, F6, F7, and F8, prepared using HPMC, showed 10.2, 13.6, 12.8, and 14.9%, respectively.

As mentioned in the literature, HPMC when used in liquisolid preparation acts as a retarding agent to prolong drug release (12); this retardation might be attributed to its gel-forming properties around the disintegrated particles (38,46). The high viscosity of HPMC around the drug particles might retard the penetration of water and thus reduce its dissolution. Also, it was previously reported that using PVP has a better dissolution rates; the main reason of this might be attributed to its crystal growth inhibition mechanism.

Changing the concentration of the viscosity increasing agent (Fig. 3b) was found to significantly affect the percent of SM dissolved from the prepared capsules ( $p < 0.05$ ), using 40% PVP was found to significantly increase the percent SM dissolved, as in F1 and F3 that were prepared using 40% PVP compared to F2 & F4 that were prepared using 20% PVP, giving %  $Q_{5 \text{ min}}$  20.4, 26.9, 17.8, and 22.4%, respectively, and %  $Q_{60 \text{ min}}$  of 80, 98, 78.3, and 88.05%, respectively. This significant ( $p < 0.05$ ) increase might be reckoned to the hydrophilic nature of PVP as a polymer, which might help to quicken the water sorption rate (41). This significant ( $p < 0.0001$ ) increase was explained by Jaipakdee *et al.* (41), who used the liquisolid technique to prepare tablets containing oleoresin-like crude extract of *C. comosa* to improve the dissolution profiles of its major compounds, and found that 20% PVP gave a significant ( $p < 0.05$ ) higher mean dissolution time (MDT) over that prepared with 30% PVP, the higher the MDT, the slower the release rate (47). Also, changing the concentration of HPMC from 20 to 40% significantly affected the percent of SM dissolved, using

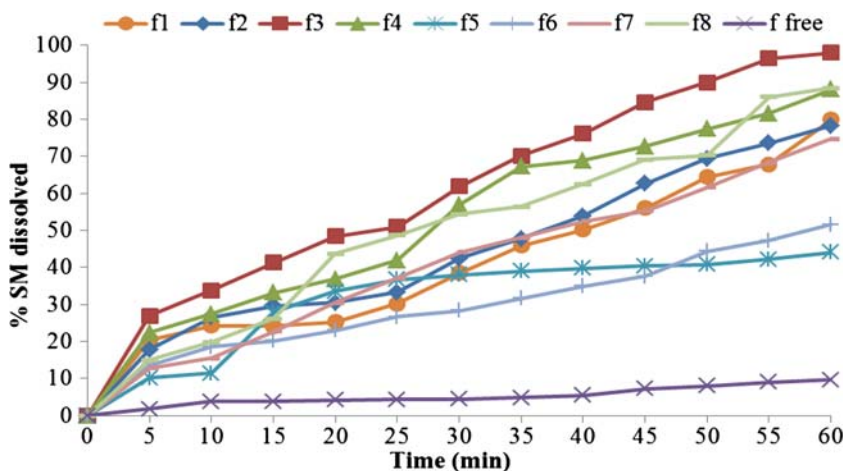


**Fig. 2.** The dissolution of SM from the different prepared liquisolid capsules compared to the dissolution of equivalent amount of free drug

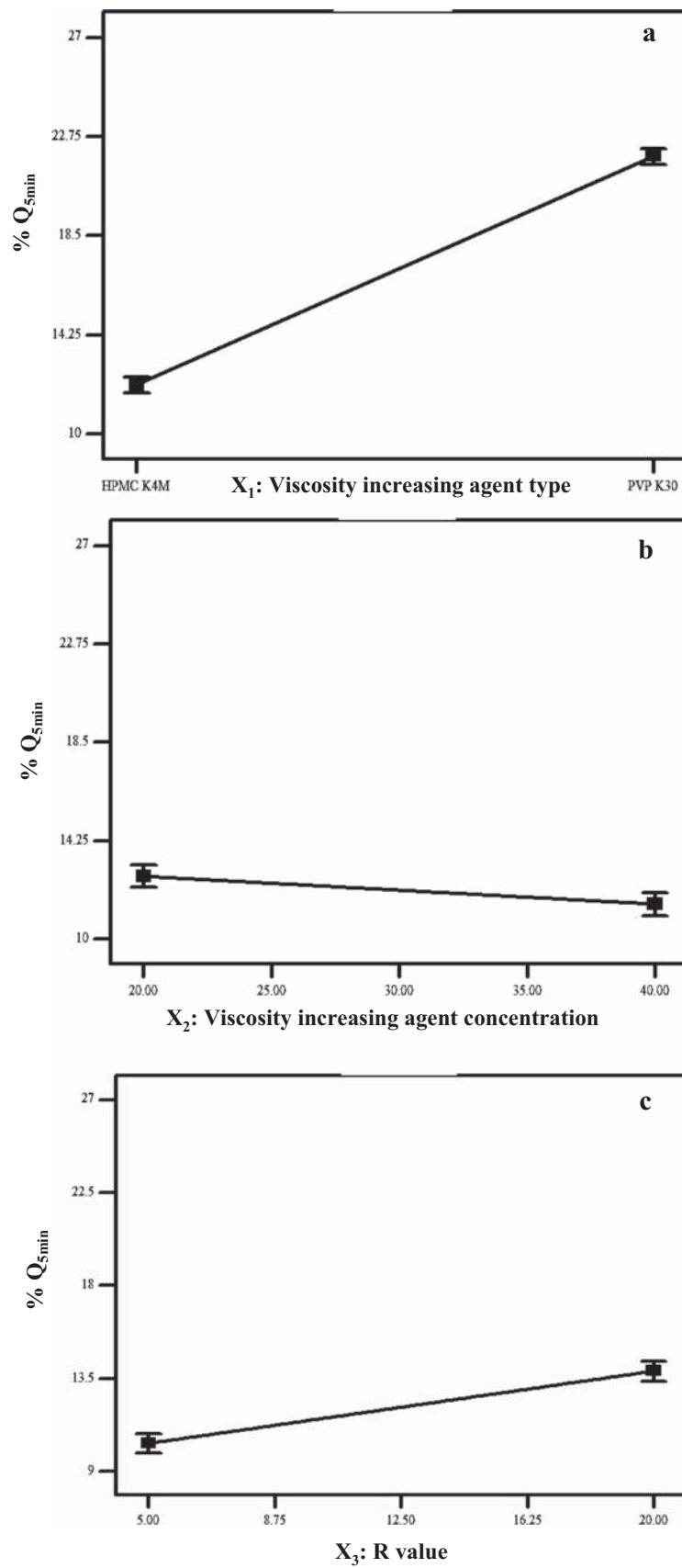


**Fig. 3.** The effect of **a** X<sub>1</sub> (viscosity increasing agent type), **b** X<sub>2</sub> (viscosity increasing agent concentration), and **c** X<sub>3</sub> (R value) on % Q<sub>5min</sub>



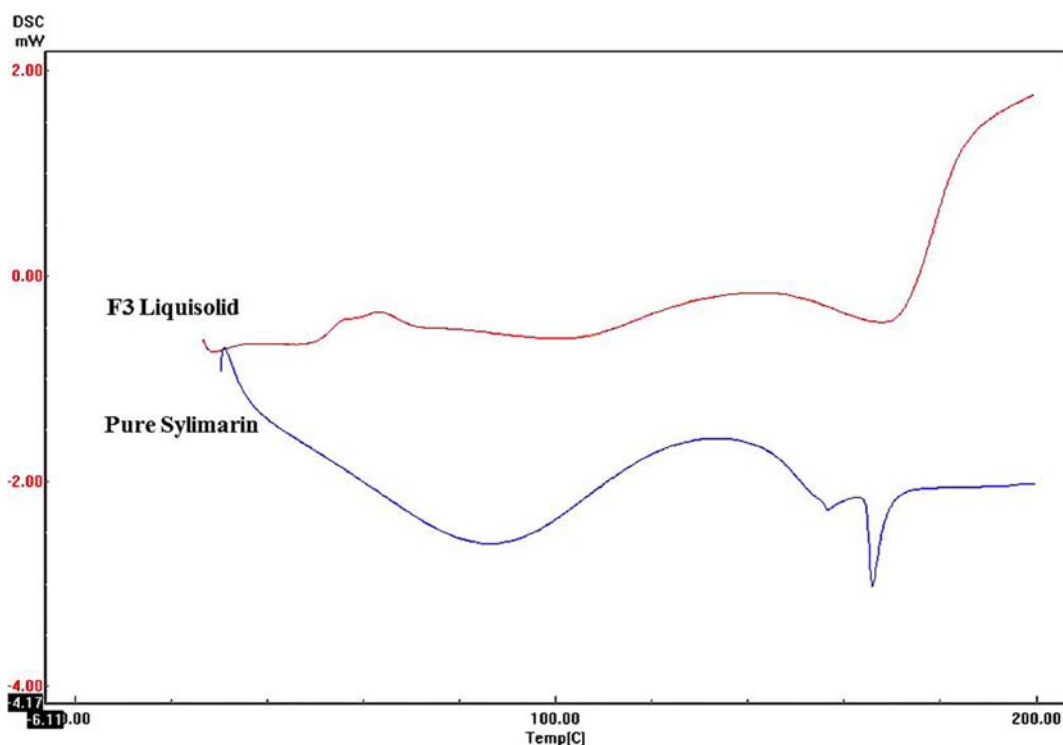


Fig. 4. DSC thermogram of pure SM and F3 liquesolid compact

higher concentration of HPMC showed an obvious decrease ( $p < 0.05$ ) in the percent of SM dissolved; this could be reckoned to the slow hydration and erosion of HPMC (48).

From Fig. 3c, it was noticed that using higher R ratios caused an obvious ( $p < 0.0001$ ) increase in the percent of SM dissolved, F3 and F4 with R value of 20 showed %  $Q_{5 \text{ min}}$  of 26.9

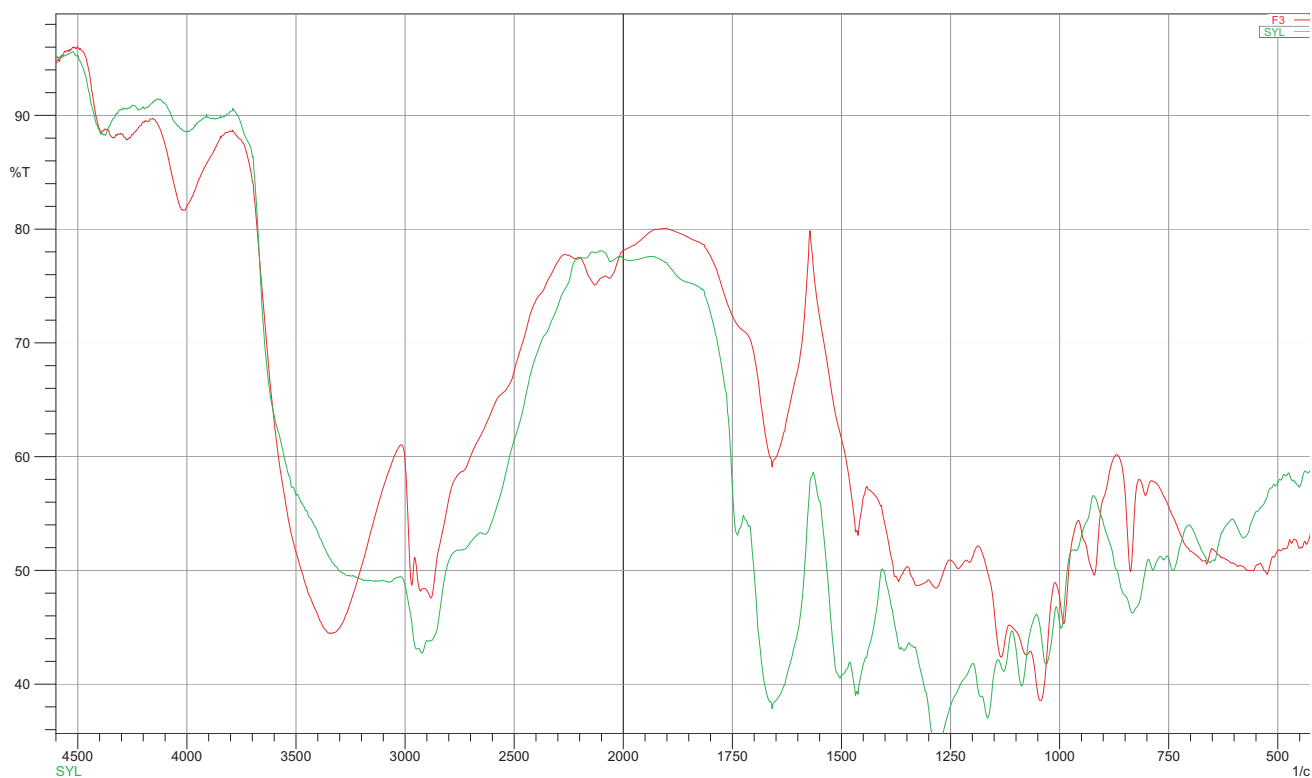
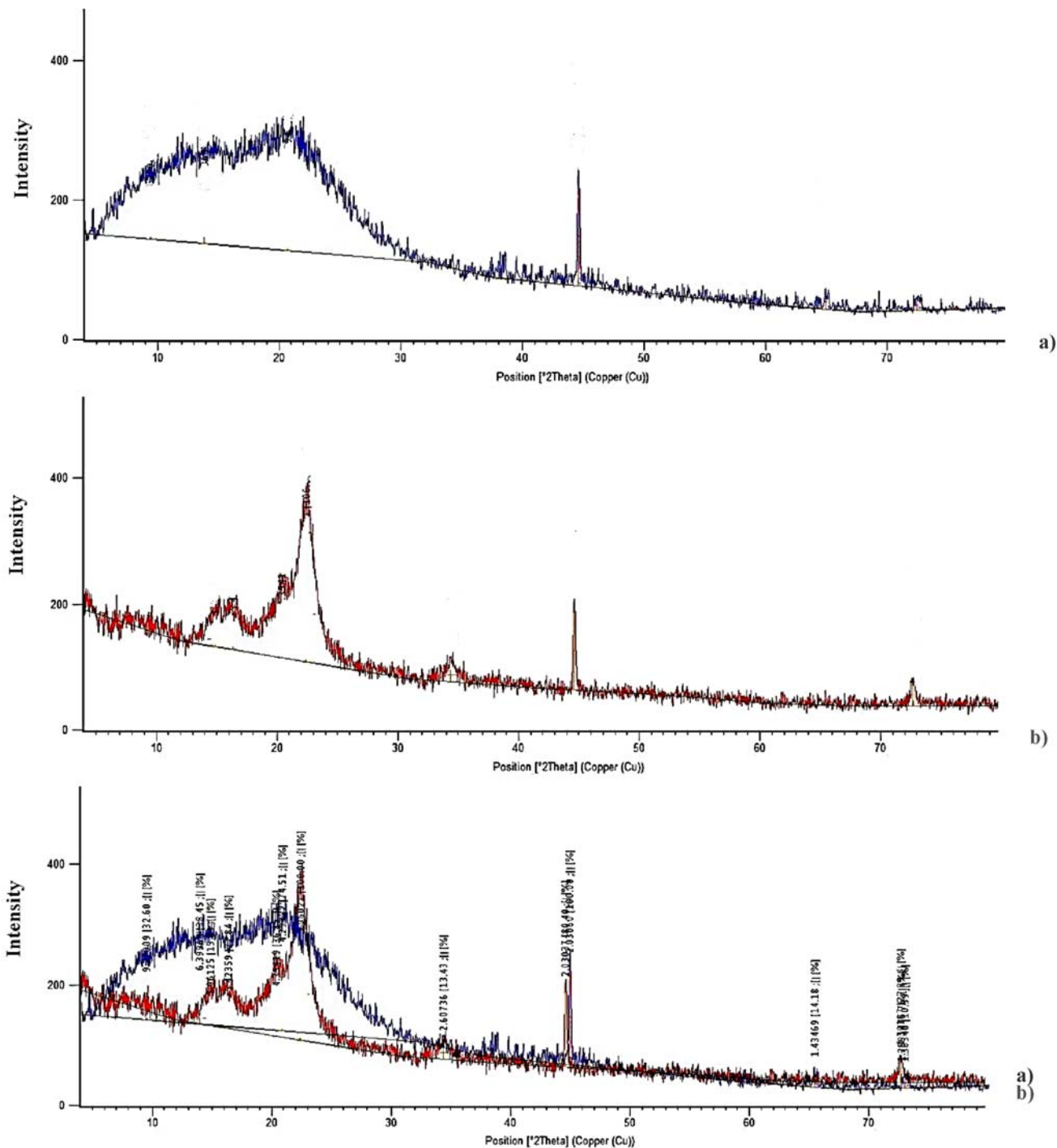


Fig. 5. FT-IR spectra of (a) pure SM and (b) F3 liquesolid compact

and 22.4%, respectively, with %  $Q_{60 \text{ min}}$  of 98 and 88%, respectively, compared to F1 and F2 with R value of 5 which showed %  $Q_{5 \text{ min}}$  of 20.4 and 17%, respectively, and %  $Q_{60 \text{ min}}$  of 80 and 78.3%, respectively; the same observation was found in F7 and F8 with higher R value = 20. This could be explained due to the possession of liquisolid formulae a low R values which contain small amounts of cellulose, and large quantities of fine drug loaded silica, and the amounts of liquid medication per powder were relatively higher. On the other hand, liquisolid formulae possessing

high R values contain low liquid/powder ratios, high presence of cellulose, and low presence of silica; this could be directly associated with enhanced wicking, disintegration, and de-aggregation properties (49).

From the previous results and according to the factorial design study, F3 showed the highest desirability = 0.903, giving the lowest angle of repose = 19 and the highest %  $Q_{5 \text{ min}}$  = 26.9%, therefore was selected as the most optimum formula which was subjected to further investigations.



**Fig. 6.** X-ray diffractograms of **a** pure SM (blue line) and F3 liquisolid compact (red line). **b** An overlay XRD for pure SM (blue line) and F3 liquisolid compact (red line)

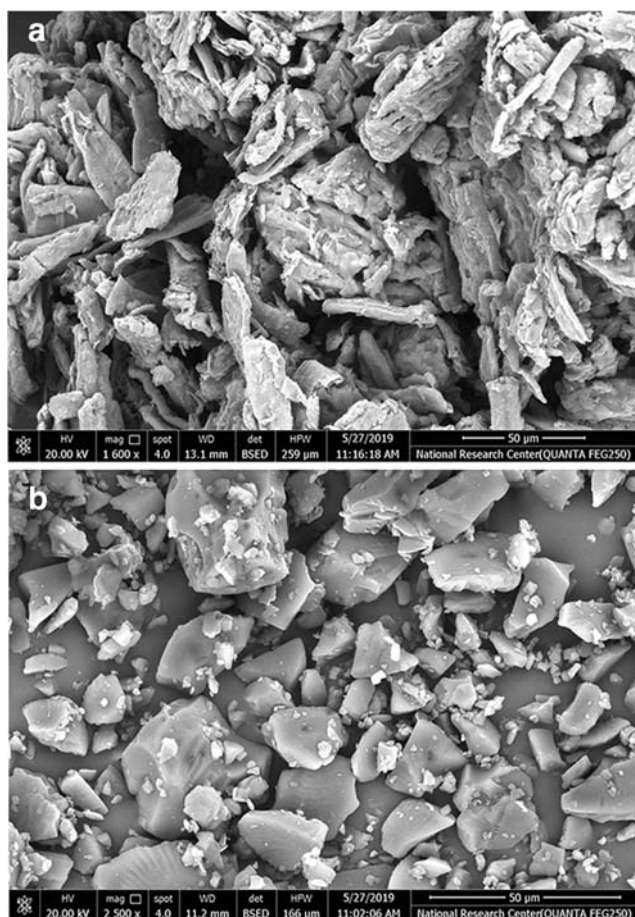


**Fig. 7.** Topographic visualization of **a** pure SM and **b** F3 by SEM

### Characterization of the Selected SM Liquisolid Free-Flowing Powder

#### DSC

The interaction between SM and excipients in liquisolid compact was determined by DSC. Figure 4 shows the thermal behavior of pure SM and F3 liquisolid formula. Pure SM showed a characteristic peak at 166°C (50), which is indicative for its crystalline nature. Furthermore, the thermal behavior of F3 liquisolid compact showed a shifted broad peak, which indicates the transformation of SM from its crystalline state to another amorphous state (51).

#### FT-IR

The FT-IR spectrum of pure SM and F3 liquisolid compact is displayed in Fig. 5. The FT-IR spectrum of pure SM revealed several peaks corresponding to flavonolignans. SM showed peaks at 1680  $\text{cm}^{-1}$  corresponding to (C=O) carbonyl vibrations and 1450  $\text{cm}^{-1}$  attributed to the symmetric aromatic ring stretching vibration (C=C ring). The appearing peak at 1045  $\text{cm}^{-1}$  indicated the benzopyran ring with simultaneous presence of out plane -CH deformations at 845  $\text{cm}^{-1}$ . All of these indicate the IR spectra of SM. FT-IR spectra of the F3 formula showed the main characteristic peaks without shifting, thus indicating the absence of interaction between SM and excipients.

#### XRD

The X-ray of SM, as well as F3 liquisolid compact, is represented in Fig. 6a and b. The diffractogram of pure SM showed intense peaks indicative for its crystallinity. However, in case of F3 liquisolid compact diffractogram, a new solid phase with low crystallinity was shown, indicating the inclusion of SM inside the liquisolid form (more water soluble). A reduced number of signals of markedly low intensity are noticeable in F3, indicating its partially amorphous form compared to the free molecules (52,53).

#### (SEM) Topographic Visualization

The topographic visualization of pure SM is shown in Fig. 7a, revealing regular crystalline surface of particles, while the selected F3 liquisolid shown in Fig. 7b revealed irregular shaped aggregates, confirming the complete disappearance of SM crystals and therefore supporting its transformation from crystalline to amorphous state which is totally solubilized in liquisolid system.

### Investigating the Cardioprotective Efficacy of SM in Isoproterenol Prompting Myocardial Infarction in Rats

Table IV reveals an obvious elevation in LDH, CK-MB, cTnT, and BNP in the 2nd group as compared with control. The administration of SM, F3 liquisolid, and propranolol showed a significant decrease in LDH, CK-MB, cTnT, and BNP levels relative to isoproterenol-treated rats ( $p < 0.05$ ). Table V reveals an obvious increase in plasma IL-10, VEGF, and TGF- $\beta$ 1 levels ( $p < 0.05$ ) in the 2nd group as compared with control. The administration of SM, F3 liquisolid, and

**Table IV.** Effect of Pure SM, F3 Liquisolid Compact, and Propranolol on Plasma “LDH,” “CK-MB,” “cTnT,” and “BNP” in Rats

No.	Groups	LDH (U/L)	CK-MB (U/L)	cTnT (U/L)	BNP (ng/mL)
(I)	Normal	409.6 ± 10.82a	26.67 ± 2.30a	0.09 ± 0.01a	0.68 ± 0.06a
(II)	Control positive ISO (85 mg/kg)	511.11 ± 11.82b	40.46 ± 3.62b	0.84 ± 0.10b	3.17 ± 3.17b
(III)	Propranolol (10 mg/kg) + isoproterenol (85 mg/kg)	404.75 ± 5.5a	33.89 ± 2.61a	0.31 ± 0.22a	1.93 ± 0.61a
(IV)	Silymarin (100 mg/kg) + isoproterenol (85 mg/kg)	459.47 ± 17.63a	28.71 ± 4.47a	0.28 ± 0.30a	2.61 ± 0.69a
(V)	F3 (100 mg/kg) + isoproterenol (85 mg/kg)	420.11 ± 15.76a	22.32 ± 2.15a	0.09 ± 0.02a	1.35 ± 0.31a

Data shown are mean average value (± SD),  $n = 8$ . Data followed by the same letter are non-significantly different ( $p \leq 0.05$ )

**Table V.** The Impress of Pure SM, F3 Lquisolid Compact, and Propranolol on Serum “IL-10,” “TGF-β1,” and “VEGF” in Rats

No.	Groups	IL-10 (pg/mL)	TGF-β1 (pg/mL)	VEGF (pg/mL)
(I)	Normal	67.88 ± 5.80a	85.91 ± 4.30 a	9.75 ± 1.77a
(II)	Control positive ISO (85 mg/kg)	117.26 ± 9.36b	233.92 ± 11.36b	21.06 ± 3.51b
(III)	Propranolol (10 mg/kg) + isoproterenol (85 mg/kg)	78.37 ± 2.46a	106.04 ± 10.90a	12.73 ± 1.13a
(IV)	Silymarin (100 mg/kg) + isoproterenol (85 mg/kg)	90.95 ± 3.02a	113.44 ± 6.59a	13.53 ± 1.83a
(V)	F3 (100 mg/kg) + isoproterenol (85 mg/kg)	75.09 ± 7.00a	86.91 ± 7.12a	9.70 ± 1.19a

Data shown are mean average value (± SD),  $n = 8$ . Data followed by the same letter are non-significantly different ( $p \leq 0.05$ )

**Table VI.** The Impress of Pure SM, F3 Lquisolid Compact, and Propranolol on Cardiac “SOD,” “MDA,” and “Akt-1” in Rats

No.	Groups	SOD (U/mg protein)	MDA (nmol/mg protein)	Total Akt-1 (ng/mg protein)
(I)	Normal	89.38 ± 9.82a	2.21 ± 0.62 a	0.56 ± 0.09a
(II)	Control positive ISO (85 mg/kg)	20.84 ± 3.40b	5.85 ± 0.72b	0.29 ± 0.08b
(III)	Propranolol (10 mg/kg) + isoproterenol (85 mg/kg)	59.13 ± 5.17c	2.84 ± 0.50a	0.53 ± 0.06a
(IV)	Silymarin (100 mg/kg) + isoproterenol (85 mg/kg)	68.21 ± 5.40d	3.62 ± 3.02c	0.52 ± 0.12a
(V)	F3 (100 mg/kg) + isoproterenol (85 mg/kg)	75.52 ± 5.86a	2.27 ± 0.44a	0.66 ± 0.17c

Data shown are mean average value (± SD),  $n = 8$ . Data followed by the same letter are non-significantly different ( $p \leq 0.05$ )

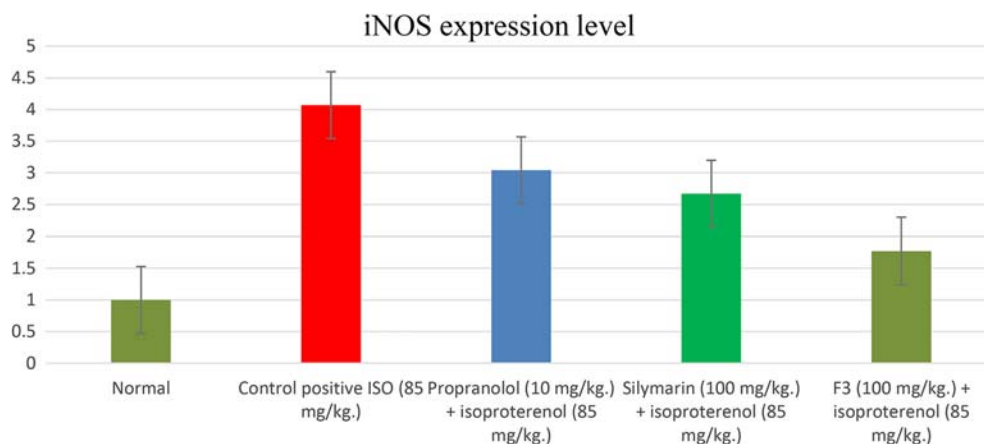


**Fig. 8.** Effect of pure SM, F3 liquisolid, and propranolol on cardiac “iNOS” in rats. The results are expressed in terms of fold increase or decrease considering the negative control one

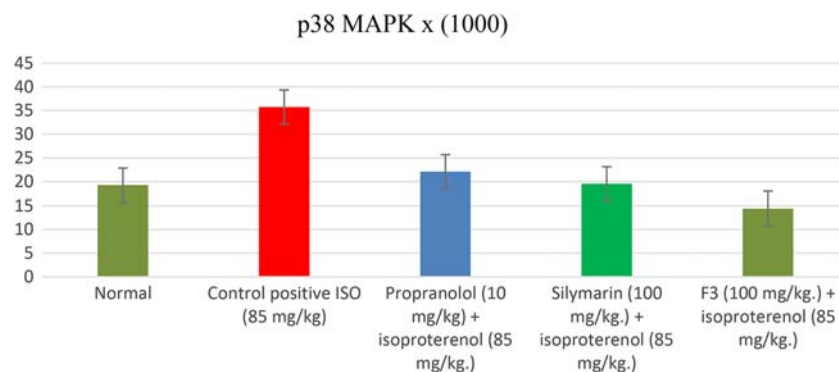


**Fig. 9.** Effect of pure SM, F3 liquisolid, and propranolol on cardiac phosphospecific “p38-MAPK” in rats. The results are expressed in terms of fold increase or decrease considering the negative control one



**Fig. 10.** An agarose gel electrophoresis shows PCR products of cardiac “iNOS” (a), “p38-MAPK” (b), and beta-actin (c) in different groups

propranolol showed significantly decreased in IL-10 and VEGF as well as TGF- $\beta$ 1 levels relative to isoproterenol-treated rats ( $p < 0.05$ ).

Table VI reveals a significant reduction in heart SOD and Akt-1 as well as significant elevation of MDA levels ( $p < 0.05$ ) in the 2nd group compared with control. Administration of SM, F3 liquisolid, and propranolol showed significant increase in SOD and Akt-1 as well as significant decrease in MDA levels relative to isoproterenol treated rats ( $p < 0.05$ ) with best results in group 5. Figure 8 displays that isoproterenol promoted the iNOS protein expression as compared with control. Administration of SM, F3 liquisolid, and propranolol led to significant decrease of iNOS protein expression relative to isoproterenol-treated group of rats ( $p < 0.01$ ) with best results in group 5. Agarose gel electrophoresis images of iNOS and  $\beta$ -actin support the present results (Fig. 10).

Figure 9 shows a significant increase in the expression levels of p38 MAPK in rats treated with isoproterenol when compared with normal control group, administration of SM, F3 liquisolid, and propranolol led to statistically significant decrease of p38 MAPK protein expression relative to isoproterenol-treated group of rats ( $p < 0.01$ ) with best results in group 5. Agarose gel electrophoresis images of p38 MAPK and  $\beta$ -actin support the present results Fig. 10.

Figure 11 revealed that RT-qPCR results were employed to detect the expressions of miRNA-34a in myocardial tissues of rats in all groups. The results showed that an obvious increase in the expression levels of miRNA-34a in rats treated with isoproterenol when compared with normal control group, while the expression of miRNA-34a was downregulated in SM, F3 liquisolid, and propranolol-treated rats

relative to isoproterenol-treated group, the results of group 4 and 5 were better than that of group 3.

As a therapeutic agent, SM is well tolerated and largely free of adverse effects (54). The effect of its flavolignans and other polyphenolic constituents is due to scavenging of both free radicals and reactive oxygen species (55). SM received attention because of its benefits gained indirectly from its hepatoprotective effects. These benefits include mostly anti-cancer effects, anti-inflammatory hypocholesterolemic, and renal protection (56).

In the present investigation, increased levels of LDH, CK-MB, cTnT, and BNP in the isoproterenol-treated group of rats were observed when compared with control group. Marked elevations in the level of these markers in the serum of the control ischemia-reperfusion group indicate the existence of membrane damage compared with control. Treatment with F3 liquisolid resulted in reduction over SM in the levels of these markers toward near normal levels when compared with the isoproterenol-treated group.

The results of the present study demonstrated the pronounced effect of F3 liquisolid over SM in reducing IL-10, VEGF, and TGF- $\beta$ 1 levels in rat with acute myocardial infarction (AMI) induced by isoproterenol. It has been shown that F3 liquisolid and SM had a protective effect against d-galactose-induced senescence due to the allowing of cellular oxidoreductase activities and preventing NF- $\kappa$ B activation and ROS production (57). Also, studies in rats showed that SM markedly inhibited the caspase-3-mediated tubular cell apoptosis and minimized the NADPH oxidase, iNOS, and NF- $\kappa$ B overexpression (58).

In a model of experimental ischemic stroke in male rats, SM significantly downregulated IL-10, VEGF, and TGF- $\beta$ 1 in ischemic brain tissue after stroke (59). Protective effect of F3 liquisolid and SM in the rat model of cerebral ischemia was attributed to reduced expression of the NF- $\kappa$ B protein and NF- $\kappa$ B mRNA in the brain (60). F3 liquisolid and SM were shown to have NF- $\kappa$ B inhibiting effects. For example, mRNA and protein expressions of NF- $\kappa$ B were significantly upregulated in d-galactosamine-induced hepatotoxicity and treatment with F3 liquisolid and SM significantly downregulated these gene expressions (61).

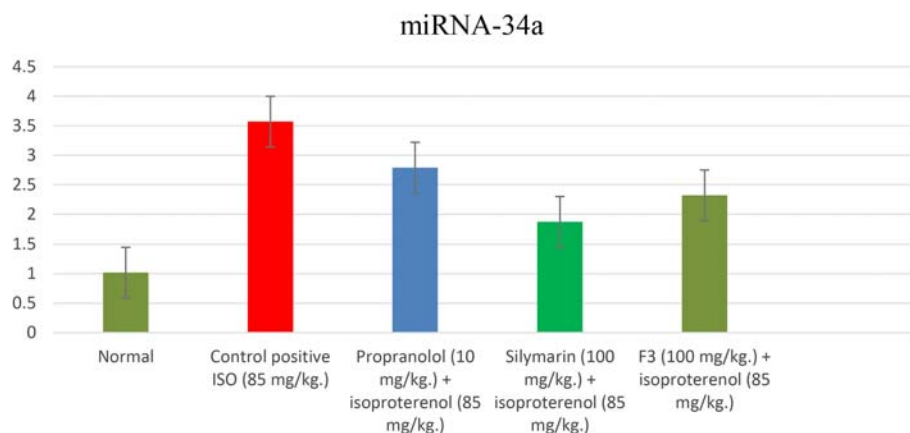


**Fig. 11.** Effect of pure SM, F3 liquisolid, and propranolol on cardiac microRNA-34a (miR-34a) in rats. The results are expressed in terms of fold increase or decrease considering the negative control one



Experimental results showed that after AMI, myocardial antioxidant ability was decreased, the level of oxidative stress was elevated, myocardial apoptosis was aggravated, and it was obvious in Akt-1, SOD, and MDA levels (62). In this study, the levels of MDA, SOD, and Akt-1 in rats with AMI induced by isoproterenol were significantly restrained by treatment with F3 liquisolid and SM with better results with F3 liquisolid.

SM was examined for its protective effect against beta-adrenergic agonist isoproterenol-induced injury in cultured rat cardiac myocytes (63). It was shown that F3 liquisolid and SM addition caused an increase in SOD activity and upregulation of mitochondrial membrane potential with prevention of mitochondrial dysfunction and cell injury (64). Both F3 liquisolid and SM fully mitigated the rise in ROS formation in perfused rat hepatocytes. In addition, studies on isolated liver mitochondria showed that low dose of SM reduced ROS production linked to the electron transfer chain activity (65).

Myocardial ischemia and hypoxia lead to the activation of P38MAPK, nuclear translocation starting iNOS protein expression, and the secretion of TNF- $\alpha$  which can activate p38MAPK to induce apoptosis, and constitutes a positive feedback path, resulting in impaired cardiac function, amplifying the inflammatory cascade and thus causing the death of heart cells, so as to achieve cell death. In myocardial cells, IL-1 $\beta$  can induce P38MAPK activation and increase its activity, thereby inducing cardiac endothelial cell death and stimulating neutrophil function, leading to the increase of TNF- $\alpha$  and the accumulation of neutrophils in myocardial tissue, which causes damage to myocardial tissue (66).

The anti-inflammatory effects of polyphenols have been attributed to the prevention of canonical NF- $\kappa$ B pathway. The canonical NF- $\kappa$ B pathway is stimulated by proinflammatory signals, leading to degradation of I $\kappa$ B kinase (IKK) complex releasing NF- $\kappa$ B into the nucleus, resulting in inflammatory response (67). It was stated that kaempferol prevented the phosphorylation of insulin receptor substrate 1 (IRS-1), IKK $\alpha$ , and IKK $\beta$ , accompanied by decreasing NF- $\kappa$ B in nucleus and cytoplasm and reducing TNF- $\alpha$  and IL-6 levels in insulin resistance and type 2 diabetes mellitus mice (68).

Other polyphenols such as curcumin, morin, oligonol, and quercetin also inhibited NF- $\kappa$ B pathway in non-alcoholic fatty liver disease (NAFLD). MAPK, a class of serine/threonine protein kinase widely expressed in mammalian cells, including extracellular signal-regulated kinases (ERKs), c-Jun N-terminal kinases (JNK), and p38MAPK, is also closely related to inflammation. MAPK, especially JNK and p38MAPK, is the action mechanism of some polyphenols for treating NAFLD. For example, cocoa flavonoids and apple polyphenols revealed advantageous results on redox balance and insulin resistance by targeting MAPKs in the context of NAFLD (69,70).

In our study, we found that F3 liquisolid followed by SM showed a significantly downregulated P38MAPK protein expression in rats with AMI induced by isoproterenol. Usta *et al.* (71) concluded that treatment with polyphenols suppresses migration, invasion, and metastasis through p38MAPK signaling pathway in human cardiac tissue.

Studies suggested that miRNAs are involved in heart development and stem cell differentiation through

translational repression (72). Studies indicated that miR-21a participated in the cell autophagy regulatory mechanism (73). Moreover, miR-34a inhibits cell autophagy by regulating the activity of TNF- $\alpha$  (74). In addition, all miRNAs of miR-21, miR-34a, and miR-214 are all involved in the regulatory mechanism of myocardial fibrosis (75). The results of this study cleared that under the stimulation of high-concentration isoproterenol, significant fibrosis was present in the myocardium, significant up regulation of the expression levels of miR-34a in myocardial tissues were found, as well as decrease of autophagy in myocardial tissues. The present study suggested that oral administration of F3 liquisolid and SM downregulated miR-34a expression in rats treated with isoproterenol. No available data about the mechanism of SM activity on miR-34a gene expression. Studies have confirmed that plant flavonoids have biological advantages such as antioxidant, anti-inflammatory, antitumor, and antiatherosclerotic properties (76). The flavonoid reduced carcinogenesis causing apoptosis of breast cancer cells partially through miR-21 and miR-34a association.

## CONCLUSION

This study clearly demonstrated the pronounced efficacy of F3 liquisolid administration to rats with myocardial infarction induced by isoproterenol. F3 possessed a noticeable cardioprotection by reducing the modifications in the levels of VEGF, SOD, MDA, TGF- $\beta$ 1, IL 10, iNOS, and p38 MAPK over pure SM as a result of improving its discounted water solubility, oral absorption, and bioavailability in liquisolid compact.

## COMPLIANCE WITH ETHICAL STANDARDS

All procedures were performed in accordance with guidelines established by the animal care and use approved by research ethical committee of O6U, Faculty of Pharmacy, Egypt.

**Conflict of Interest** The authors declare that they have no conflicts of interest.

## REFERENCES

1. Yousaf AM, Malik UR, Shahzad Y, Mahmood T, Hussain T. Silymarin-laden PVP-PEG polymeric composite for enhanced aqueous solubility and dissolution rate: preparation and in vitro characterization. *J Pharm Anal.* 2019;9:34–9.
2. Sornsuvit C, Hongwiset D, Yotsawimonwat S, Toonkum M, Thongsawat S, Taesotikul W. The bioavailability and pharmacokinetics of silymarin SMEDDS formulation study in healthy Thai volunteers. *Evid Based Complement Alternat Med.* 2018;1–7.
3. Javed S, Kohli K, Ali M. Reassessing bioavailability of silymarin. *Alternative Medicine Rev.* 2011;16:239–49.
4. Taleb A, Ahmad KA, Ihsan AU, Qu J, Lin N, Hezam K, et al. Antioxidant effects and mechanism of silymarin in oxidative stress induced cardiovascular diseases. *Biomed Pharmacother.* 2018;102:689–98.
5. Surai PF. Silymarin as a natural antioxidant: an overview of the current evidence and perspectives. *Antioxidants (Basel).* 2015;4(1):204–47.

6. Rahimia R, Karimia J, Khodadadia I, Tayebinia H, Kheiripourb N, Hashemniac M, et al. Silymarin ameliorates expression of urotensin II (U-II) and its receptor (UTR) and attenuates toxic oxidative stress in the heart of rats with type 2 diabetes. *Biomed Pharmacother*. 2018;101:244–50.
7. Chen L, Hu JY, Wang SQ. The role of antioxidants in photoprotection: a critical review. *J Am Acad Dermatol*. 2012;23:231–40.
8. Alcantara EH, Shin MY, Sohn HY, Park YM, Kim T, Lim JH, et al. Indole alkaloids from *Catharanthus roseus*: bioproduction and their effect on human health. *Molecules*. 2015;20:2973–3000.
9. Eleni T, Kateřina P, Haralambos S, Fragiskos K, Vladimir K. Bioavailability of silymarin flavonolignans: drug formulations and biotransformation. *Phytochem Rev*. 2014;13:1–18.
10. Di Costanzo A, Angelico R. Formulation strategies for enhancing the bioavailability of silymarin: the state of the art. *Molecules*. 2019;24(11):2155.
11. Piazzini V, D'Ambrosio M, Luceri C, Cinci L, Landucci E, Bilia AR, et al. Formulation of nanomicelles to improve the solubility and the oral absorption of silymarin. *Molecules*. 2019;24:1688.
12. Lu M, Ding P. Lquisolid technique and its applications in pharmaceuticals. *Asian J Pharm Sci*. 2017;12:115–23.
13. Javadzadeh Y, Jafari-Navimipour B, Nokhodchi A. Lquisolid technique for dissolution rate enhancement of a high dose water-insoluble drug (carbamazepine). *Int J Pharm*. 2007;341:26–34.
14. Soliman SM, Abdel Malak NS, El-Gazayerly ON, Abdel Rehim AA. Formulation of microemulsion gel systems for transdermal delivery of celecoxib: *in vitro* permeation, anti-inflammatory activity and skin irritation tests. *Drug Discov Ther*. 2010;4(6):459–71.
15. Balata GF. Formulation and evaluation of gliclazide in vegetable oil-based self emulsifying delivery system. *J App Pharm Sci*. 2018;8(09):023–33.
16. Sonali D, Tejal S, Vaishali T, Tejal G. Silymarin-solid dispersions: characterization and influence of preparation methods on dissolution. *Acta Pharma*. 2010;60:427–43.
17. Naveen C, Shastri N, Tadikond RR. Use of the lquisolid compact technique for improvement of the dissolution rate of valsartan. *Acta Pharma Sin B*. 2012;2:502–8.
18. Swain S, Niranjana C, Bhanaji Rao ME. *Pharmaceutical drug delivery systems and vehicles*. 1st ed. Woodhead Publishing India: Publisher; 2015.
19. Pavani E, Noman S, Syed IA. Lquisolid technique based sustained release tablet of trimetazidine dihydrochloride. *Drug invention today*. 2013;5:302–10.
20. Han X, Qi W, Dong W, Guo M, Ma P, Wang J. Preparation, optimization and *in vitro-in vivo* investigation for capsules of the choline salt of febuxostat. *Asian J Pharm Sci*. 2016;11:715–21.
21. Pharmacopoeia B. The stationery office. MD: Rockville; 2012.
22. Kamel R, Basha M. Preparation and *in vitro* evaluation of Rutin nanostructured lquisolid delivery system. *Bulletin of Faculty of Pharmacy, Cairo University*. 2013;51:261–72.
23. Panda A, Biyani DM. Studies on lquisolid system as a technique to modify the dissolution rate of nifedipine. *Am J Pharmtech Res*. 2013;3:686–98.
24. Mahmoud EA, Bendas ER, Mohamed MI. Preparation and evaluation of self-nanoemulsifying tablets of carvedilol. *AAPS PharmSciTech*. 2009;10:183–92.
25. Javadzadeh Y, Siah MR, Asnaashari S, Nokhodchi A. An investigation of physicochemical properties of piroxicam lquisolid compacts. *Pharm Dev Tech*. 2008;12:337–43.
26. Patil JS, Devi VK, Devi K, Sarasija S. A novel approach for lung delivery of rifampicin-loaded liposomes in dry powder form for the treatment of tuberculosis. *Lung India*. 2015;32(4):331–8.
27. Yang G, Zhao Y, Feng N, Zhang Y, Liu Y, Dang B. Improved dissolution and bioavailability of silymarin delivered by a solid dispersion prepared using supercritical fluids. *Asian J Pharm Sci*. 2015;10:194–202.
28. Reema O, Chandrasekhar S, Chandrakala K. Bio-tea prevents membrane destabilization during isoproterenol-induced myocardial injury. *J Microsc Ultrastruct*. 2017;5:146–54.
29. Farah N, Nasim J, Nayma S, Mohammad H. Effects of peanut (*Arachis hypogaea L.*) and its combination with propranolol in isoproterenol induced myocardial damage in rats. *J Bangladesh Soc Physiol*. 2016;11:74–9.
30. Gerhardt W, Waldenström J. Creatine kinase B-subunit activity in serum after immunoinhibition of M-subunit activity. *Clin Chem*. 1979;25:1274–80.
31. King J. The dehydrogenase or oxidoreductase. Lactate dehydrogenase. In: *Practical clinical enzymology*. London: Nostr. and Co.; 1965.
32. Nichans WH, Samulelson B. Formation of malondialdehyde from phospholipid arachidonate during microsomal lipid peroxidation. *Eur J Biochem*. 1968;6:126–30.
33. Marklund S, Marklund D. Involvement of the superoxide anion radical in the autoxidation of pyrogallol and a convenient assay for superoxide dismutase. *Eur J Biochem*. 1974;47:469–74.
34. Hentzschel CM, Sakmann A, Leopold CS. Suitability of various excipients as carrier and coating materials for lquisolid compacts. *Drug Dev Ind Pharm*. 2011;37:1200–7.
35. Jadhav NR, Pharm M, Irny PV, Patil US. Solid state behavior of progesterone and its release from Neusilin US2 based lquisolid compacts. *J Drug Deliv Sci Tech*. 2017;38:97–106.
36. Hill SW, Varker AS, Karlage K, Myrdal PB. Analysis of drug content and weight uniformity for half-tablets of 6 commonly split medications. *J Manag Care Pharm*. 2009;15(3):253–61.
37. Baranauskaitė J, Kopustinskiene DM, Masteikova R, Gajdziok J, Baranauskas A, Bernatoniene J. Effect of liquid vehicles on the enhancement of rosmarinic acid and carvacrol release from oregano extract lquisolid compacts. *Colloids Surf A Physicochem Eng Asp*. 2018;539:280–90.
38. Nokhodchi A, Aliakbar R, Desai S, Javadzadeh Y. Lquisolid compacts: the effect of cosolvent and HPMC on theophylline release. *Colloids Surfaces B Biointerfaces*. 2010;79:262–9.
39. Tiong N, Elkordy AA. Effects of lquisolid formulations on dissolution of naproxen. *Eur J Pharm Biopharm*. 2009;73:373–84.
40. Tayel SA, Soliman II, Louis D. Improvement of dissolution properties of carbamazepine through application of the lquisolid tablet technique. *Eur J Pharm Biopharm*. 2008;69:342–7.
41. Jaipakdee N, Limpongsa E, Sripanidkulchai B, Piyachaturawat P. Preparation of *Curcuma comosa* tablets using lquisolid techniques: *in vitro* and *in vivo* evaluation. *Int J Pharm*. 2018;553:157–68.
42. Sharma V, Pathak K. Effect of hydrogen bond formation/replacement on solubility characteristics, gastric permeation and pharmacokinetics of curcumin by application of powder solution technology. *Acta Pharma Sin B*. 2016;6:600–13.
43. Spireas S, Wang T, Grover R. Effect of powder substrate on the dissolution properties of methyclothiazide lquisolid compacts. *Drug Dev Ind Pharm*. 1999;25:163–8.
44. Komala DR, Janga KY, Jukanti R, Bandari S, Gopa MV. Competence of raloxifene hydrochloride loaded lquisolid compacts for improved dissolution and intestinal permeation. *J Drug Deliv Sci Tech*. 2015;30:232–41.
45. Elkadi S, Elsamaligy S, Al-Suwayeh S, Mahmoud H. The development of self-nanoemulsifying lquisolid tablets to improve the dissolution of simvastatin. *AAPS PharmSciTech*. 2017;18:2586–97.
46. Barmpalexis P, Grypioti A, Eleftheriadis GK, Fatouros DG. Development of a new aprotinant lquisolid formulation with the aid of artificial neural networks and genetic programming. *AAPS PharmSciTech*. 2018;19:741–52.
47. Varshosaz J, Tavakoli N, Kheirolah F. Use of hydrophilic natural gums in formulation of sustained-release matrix tablets of tramadol hydrochloride. *AAPS PharmSciTech*. 2006;7(1):E1–7.
48. Xu H, Liu L, Li X, Ma J, Liu R, Wang S. Extended tacrolimus release via the combination of lipid-based solid dispersion and HPMC hydrogel matrix tablets. *Asian J Pharm Sci*. 2019;14:445–54.
49. Elkordy AA, Essa EA, Dhuppada S, Jammigumpula P. Lquisolid technique to enhance and to sustain griseofulvin dissolution: effect of choice of non-volatile liquid vehicles. *Int J Pharm*. 2012;434:122–32.
50. Ghosh A, Biswas S, Ghosh T. Preparation and evaluation of silymarin b-cyclodextrin molecular inclusion complexes. *J Young Pharmacists*. 2011;3:205–10.

51. Suryawanshi VK, Gidwani B, Verma A, Dubey N, Kaur CD. Formulation and evaluation of ramipril liquisolid compact using novel carrier. *Int J Pharm Sci Res.* 2019;10:917–25.
52. Noor AD, Al-Khedairy EBH. Formulation and evaluation of silymarin as microcrystals by in-situ micronization technique. *Iraqi J Pharm Sci.* 2019;28(1):1–16.
53. Lian R, Lu Y, Qi J, Tan Y, Niu M, Guan P, et al. Silymarin glyceryl monooleate/poloxamer 407 liquid crystalline matrices: physical characterization and enhanced oral bioavailability. *AAPS PharmSciTech.* 2011;12:1234–40.
54. Morazzoni P, Bombardelli E. Silybum marianum (*Carduus marianus*). *Fitoterapia.* 1995;66:3–42.
55. Haková H, Misúrová E, Kropáčová K. The effect of silymarin on concentration and total content of nucleic acids in tissues of continuously irradiated rats. *Vet Med (Praha).* 1996;41:113–9.
56. Kang JS, Jeon YJ, Park SK, Yang KH, Kim HM. Protection against lipopolysaccharide-induced sepsis and inhibition of interleukin-1 $\beta$  and prostaglandin E2 synthesis by silymarin. *Biochem Pharmacol.* 2004;67:175–81.
57. Wang Q, Zou L, Liu W, Hao W, Tashiro S, Onodera S, et al. Inhibiting NF- $\kappa$ B activation and ROS production are involved in the mechanism of silibinin's protection against d-galactose-induced senescence. *Pharmacol Biochem Behav.* 2011;98:140–9.
58. Prabu SM, Muthumani M. Silibinin ameliorates arsenic induced nephrotoxicity by abrogation of oxidative stress, inflammation and apoptosis in rats. *Mol Biol Rep.* 2012;39:11201–16.
59. Wang C, Wang Z, Zhang X, Zhang X, Dong L, Xing Y, et al. Protection by silibinin against experimental ischemic stroke: up-regulated pAkt, pmTOR, HIF-1 $\alpha$  and Bcl-2, down-regulated Bax, NF- $\kappa$ B expression. *Neurosci Lett.* 2012;529:45–50.
60. Liu BN, Hanm BX, Liu F. Neuroprotective effect of pAkt and HIF-1  $\alpha$  on ischemia rats. *Asian Pac J Trop Med.* 2014;7:221–5.
61. Aristatile B, Al-Assaf AH, Pugalendi KV. Carvacrol suppresses the expression of inflammatory marker genes in d-galactosamine-hepatotoxic rats. *Asian Pac J Trop Med.* 2013;6:205–11.
62. Perrelli MG, Pagliaro P, Penna C. Ischemia/ reperfusion injury and cardioprotective mechanisms: role of mitochondria and reactive oxygen species. *World J Cardiol.* 2011;3:186–200.
63. Zhou B, Wu LJ, Tashiro S, Onodera S, Uchiumi F, Ikejima T. Silibinin protects rat cardiac myocyte from isoproterenol-induced DNA damage independent on regulation of cell cycle. *Biol Pharm Bull.* 2006;29:1900–5.
64. Rolo AP, Oliveira PJ, Moreno AJ, Palmeira CM. Protection against post-ischemic mitochondrial injury in rat liver by silymarin or TUDC. *Hepato Res.* 2003;26:217–24.
65. Detaille D, Sanchez C, Sanz N, Lopez-Novoa JM, Leverve X, El-Mir MY. Interrelation between the inhibition of glycolytic flux by silibinin and the lowering of mitochondrial ROS production in perfused rat hepatocytes. *Life Sci.* 2008;82:1070–6.
66. Owona BA, Njayou NF, Laufer SA, Schluesener HJ, Moundipa PF. Entada africana fraction CH(2)cl(2)/MEOH 5% inhibits inducible nitric oxide synthase and pro-inflammatory cytokines gene expression induced by lipopolysaccharide in microglia. *BMC Complement Altern Med.* 2013;13:254.
67. Zeng L, Tang WJ, Yin JJ, Zhou BJ. Signal transductions and nonalcoholic fatty liver: a mini-review. *Int J Clin Exper Med.* 2014;7:1624–31.
68. Luo C, Yang H, Tang C. Kaempferol alleviates insulin resistance via hepatic IKK/NF- $\kappa$ B signal in type 2 diabetic rats. *Int Immunopharmacol.* 2015;28:744–50.
69. Cordero-Herrera I, Martin MA, Goya L, Ramos S. Cocoa flavonoids protect hepatic cells against high-glucose-induced oxidative stress: relevance of MAPKs. *Mol Nutr Food Res.* 2015;59:597–609.
70. Xu ZR, Li JY, Dong XW. Apple polyphenols decrease atherosclerosis and hepatic steatosis in ApoE<sup>-/-</sup> mice through the ROS/MAPK/NF- $\kappa$ B pathway. *Nutrients.* 2015;7:7085–105.
71. Usta E, Mustafa M, Walker T, Ziemer G. Resveratrol suppresses apoptosis in intact human cardiac tissue - *in vitro* model simulating extracorporeal circulation. *J Cardiovasc Surg.* 2011;52:399–409.
72. Seeger FH, Tonn T, Krzossok N, Zeiher AM, Dimmeler S. Cell isolation procedures matter: a comparison of different isolation protocols of bone marrow mononuclear cells used for cell therapy in patients with acute myocardial infarction. *Eur Heart J.* 2007;28:766–72.
73. Huang Z, Wu S, Kong F, Cai X, Ye B. MicroRNA-21 protects against cardiac hypoxia/ reoxygenation injury by inhibiting excessive autophagy in H9c2 cells via the Akt/mTOR pathway. *J Cell Mol Med.* 2017;21:467–74.
74. Shao H, Yang L, Wang L, Tang B, Wang J. MicroRNA-34a protect myocardial cells against ischemiareperfusion injury through inhibiting autophagy *via* regulating TNF- $\alpha$  expression. *Biochem Cell Biol.* 2018;96:349–54.
75. Vegter EL, van der Meer P, de Windt LJ, Pinto YM, Voors AA. MicroRNAs in heart failure: from biomarker to target for therapy. *Eur J Heart Fail.* 2016;18:457–68.
76. Lee YC, Cheng TH, Lee JS, Chen JH, Liao YC, Fong Y, et al. Nobiletin, a citrus flavonoid, suppresses invasion and migration involving FAK/PI3K/Akt and small GTPase signals in human gastric adenocarcinoma AGS cells. *Mol Cell Biochem.* 2011;347:103–15.

**Publisher's Note** Springer Nature remains neutral with regard to jurisdictional claims in published maps and institutional affiliations.